Electronic Supplementary Information for

Carbon Nanospheres Hung on Carbon Nanotubes: A Hierarchical Three-Dimensional Carbon Nanostructure for High-performance Supercapacitors

Yongsheng Zhou *[a,b], Pan Jin[a], Yatong Zhou[a], and Yingchun Zhu[b]

[a]College of Chemistry and Materials Engineering, Anhui Science and Technology University, Bengbu, 233100, China

[b] Key Laboratory of Inorganic Coating Materials, Shanghai Institute of Ceramics, Chinese Academy of Sciences, Shanghai, 200050, China

E-mail: yszhou1981@gmail.com

Table of contents

Experimental Section

Synthesis of CNs/CNTs

The catalyst preparation process can be briefly described as follows: $Co(NO_3)_2 \cdot 6H_2O$ and $Mg(NO_3)_2 \cdot 6H_2O$ were mechanically mixed, ground and then calcined at 600 ^{0}C for 2h in air to decompose the precursor and yield the cluster of cobalt and magnesium oxides; the resulted powder was then reduced in H_2 (flow rate: 100 sccm) and Ar (flow rate: 300 sccm) for 30 min at 600^{0}C to form Co nanoclusters supported on MgO substrate, which was collected and used as catalyst. Co/MgO was used as the growth catalyst precursor and dimethyl sulfide was used as carbon source. Typically, a thin layer of Co/MgO catalyst was coated on an Si wafer and inserted into a horizontal quartz tubular reaction chamber. Prior to the catalytic decomposition reaction, the catalysts were pre-reduced at 400^{0}C for 1.5 h in the flow of hydrogen (99.99% purity). Then the reaction chamber was heated up to 1000^{0}C with a flow of Ar (flow rate: 700 sccm). Ar was allowed to bubble through liquid C_2H_6S to initiate the CNs/CNTs growth. After reaction for 15 min, Ar was allowed to the chamber instead of bubbling through the liquid C_2H_6S and the chamber was cooled down naturally to room temperature under the protection of Ar. The as prepared products were washed with dilute HCl aqueous solution and distilled water. In order to avoid the influence of the sample purification treatment on the morghology, the obatained samples were first characterized by scanning electron microscope (SEM), and then washed by the use of 1 mol/L HCl at 35 0C for 24 h to remove all MgO support, most Co metals on MgO support, and some Co metals pristine inside the carbon capsule. The acid-washed sample was washed further by de-ion water for five times and dried at 110 ^{0}C for 12 h. Thus, the purity of tubes is high up to 99%. Some impurities may still remained in CNTs, e.g. Co metals inside the thick carbon capsule, do not influence the performance of supercapacitor in short time.

Synthesis of CNTs

The CNTs material was synthesised in a way limilar to that for the CNs/CNTs, but H_2 (50 sccm) was was switched to bubble through C_2H_6S to initiate the CNT growth. After growth for 15 min, the H_2 flow was stopped and the chamber was cooled down to room under the protection of Ar.

Characterization

The morphology and the microstructure of the as-synthesized product were examined using scanning electron microscopy (SEM), and transmission electron microscopy (TEM, JEM2010F). Chemical composition analysis was performed by an energy dispersive X-ray spectrometer equipped with a JEOL 2010 TEM instrument. Raman spectra were recorded on the Lab RAMHR Raman spectrometer using laser excitation at 514.5 nm from an argon ion laser source. Typical X-ray diffraction (XRD) patterns (Rigaku P/max 2200VPC) were recorded with Cu Kα radiation. Brunauer-Emmett-Teller (BET) surface areas and porosities of the products were determined by nitrogen adsorption and desorption using a Micromeritics ASAP 2020 analyzer.

Electrochemical Characterization

The preparation of electrode and analytical measurements of electrochemical properties are described as follows. The as-fabricated CNs/CNTs composite or CNTs were pressed into electrode films using standard mold with a pressure of 10MPa. The aqueous electrolyte based

supercapacitor: three-electrode system was carried out where CNs/CNTs or CNTs film was used as working electrode, platinum plate was used as the counter electrode, Ag/AgCl was employed as the reference electrode, and electrolyte was 1M H_2SO_4 solution. The organic electrolyte based supercapacitor: two-electrode system was carried out where two as-prepared CNs/CNTs nanocomposite electrodes separated by a porous paper of 50 μm, and organic electrolyte was 1 M $EMIBF_4$. The cyclic voltammetry (CV), and galvanostatic charge-discharge measurements were carried out by an electrochemical workstation (CHI 660D).

Figure S1 is the XRD pattern of CNs/CNTs. There is a broad peak at 2θ= ca. 24.8 that corresponds to the (002) diffraction of graphite. The surface area and porous structure of the obtained CNs/CNTs were investigated by means of nitrogen sorption technique.

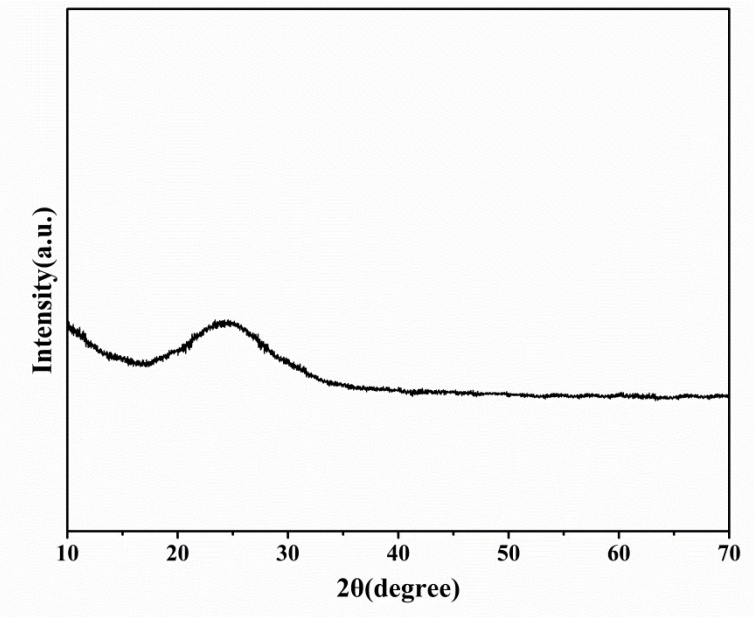

Figure S1. XRD spectroscopic of the CNs/CNTs.

The graphitization degree of the as-prepared CNs/CNTs is examed by Raman measurement (Figure S2). A characteristic peak at approximate 1350 cm^{-1} in Raman spectra can be clearly observed, which corresponds to the D-band and suggests the presence of disordered carbon structure. And the peak at about 1580 cm^{-1} is related to the G-band denoting the ordered graphite lattice of carbon material. The measured ID/IG ratio is calculated to be 0.72, indicating that the obtained CNs/CNTs exist in the more graphitic form. However, there was no peak related to the C=C stretch in (S2)C=C(S2) configuration at around 1445 cm^{-1}, suggesting that there was no C/S polymer coexists in the as-prepared CNs/CNTs products.

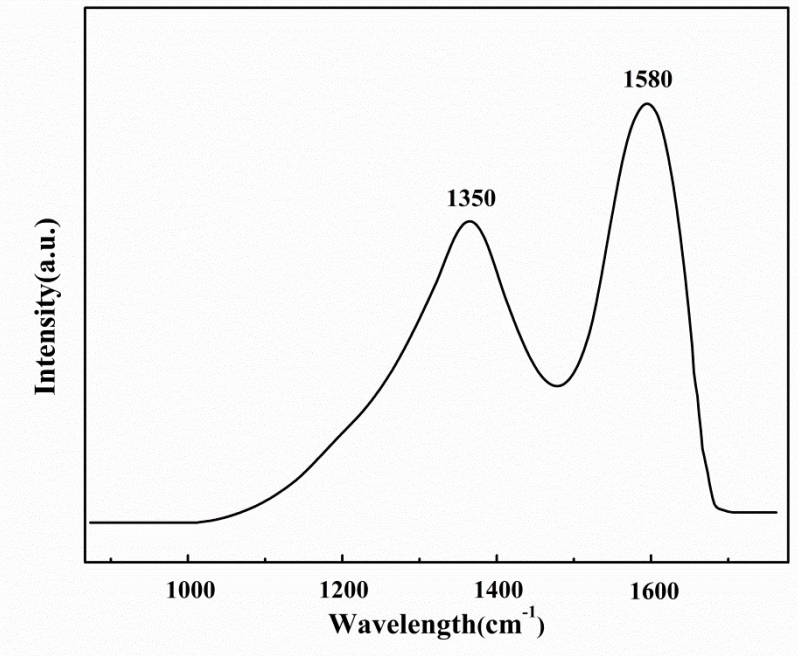

Figure S2. Raman spectroscopic of the CNs/CNTs.

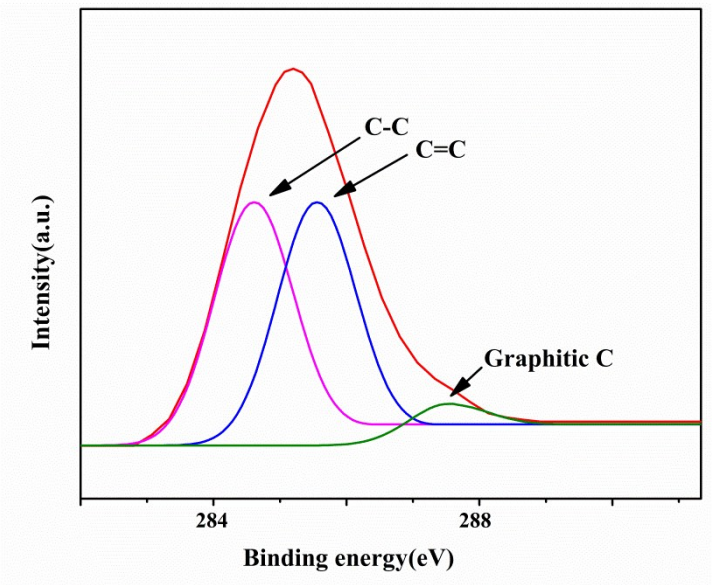

Figure S3 High-resolution XPS C1s spectrum of CNs/CNFs.

The Nitrogen adsorption-desorption isotherms and corresponding pore size distribution curves are shown in Figure S4. The as-prepared CNs/CNTs composites exhibit I-type adsorption-desorption isotherms with strong steep increase of N_2 adsorption at relative low pressure, demonstrating the existence of high microporosity in Figure S4a. Obviously, an inconspicuous hysteresis loop could be observed in the P/P_0 range of 0.5−1.0, indicating the presence of mesopores, which is further identified in the pore distribution (Figure S4b). The specific surface area of CNs/CNTs is 1476.5 m^2 g^{-1}. The pore size distribution of the CNs/CNTs is shown in Figure S4b which shows that the CNs/CNTs possess micropores and a portion of mesopores. The inset pore size distribution curves shows the magnified pore distributions in the micropore regions.

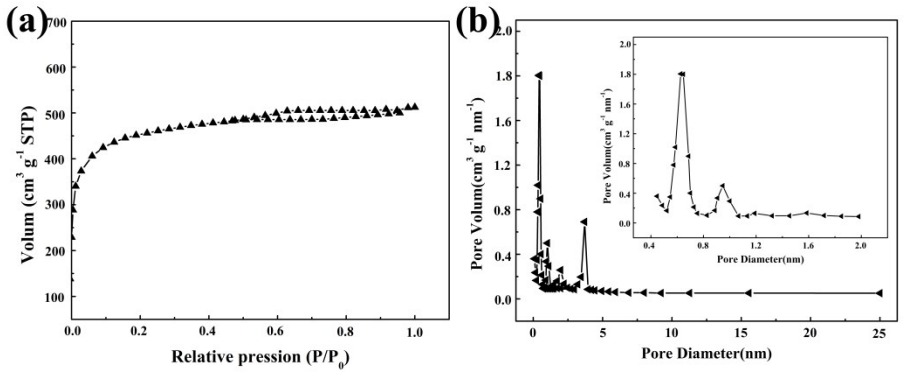

Figure S4. (a) Nitrogen adsorption-desorption isotherms and (b) pore size distribution of CNs/CNTs (inset shows the magnified pore distributions in the micropore regions).

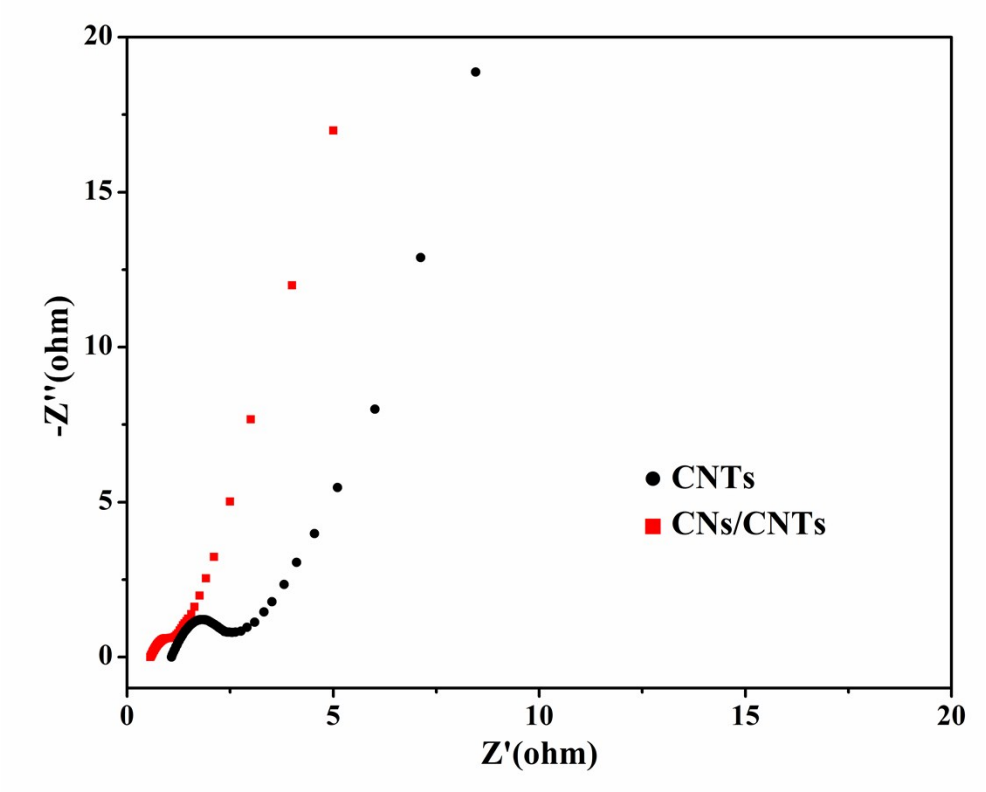

Figure S5. EIS measurements of CNs/CNTs and CNTs-based EDL supercapacitors.

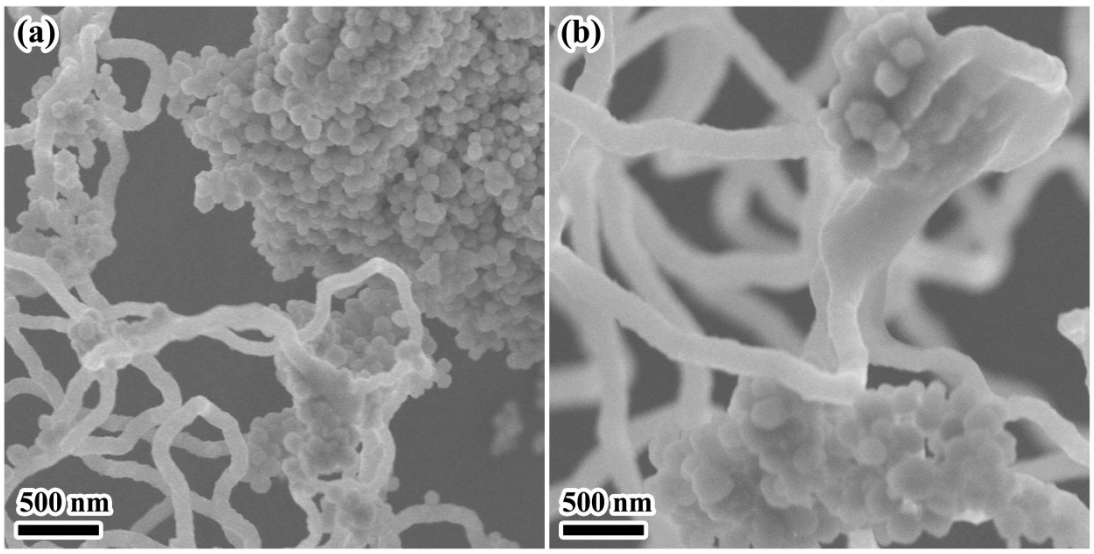

Figure S6. The SEM image of CNs/CNTs before (a) and after (b) 10 000 cycling tests.

Table S1| Specific capacitance and energy density values of different CNT-based materials for supercapacitors.

Materials	Capacitance	Energy density	References
CNT/graphene	120 F g^{-1} in 1.0 M H_2SO_4		1
Activated carbon wrapped CNT buckypaper	100 F g^{-1} in 6 M KOH		2
CNT/PEDOT	179 F cm^{-3} in H_3PO_4/PVA	1.4 mWh cm^{-1}	3
CNT/PPY	184 F g^{-1} in KCl solution		4
CNT/CoS	796 F g^{-1} in 6 M KOH	61 Wh kg^{-1}	5
CNT sponge	20 F g^{-1} in 6 M KOH		6
Macro-/meso-porous CNT sponge	150 F g^{-1} in 6 M KOH		6
CNT supported graphene aerogel	169.3 F g^{-1} in 6 M KOH		7
VACNTs/CNFs	213 F g^{-1} in NaOH	70.7 Wh kg^{-1}	8
CNTs/PANI hydrogel	315 F g^{-1} in H_3PO_4/PVA		9
MoS_2 @rGO-CNT	13.7 mF cm^{-2}	5.6 mWh cm^{-3}	10
CNT@micro-carbon	209 F g^{-1} in 6 M KOH		11
Our work	243.7 F g^{-1} in H_2SO_4	61.2 Wh kg^{-1}	

References

1. D. S. Yu, L. M. Dai. Self-assembled graphene/carbon nanotube hybrid films for supercapacitors. *J. Phys. Chem. Lett*. 2010, **1**, 467-470.
2. H. Y. Chen, J. T. Di, Y. Jin, M. H. Chen, J. Tian, Q. W. Li. Active carbon wrapped carbon nanotube buckypaper for the electrode of electrochemical supercapacitors. *J. Power Sources* 2013, **237,** 325-331.

3. J. A. Lee, M. K. Shin, S. H. Kim, H. U. Cho, G. M. Spinks, G. G. Wallace, M. D. Lima, X. Lepro, M. E. Kozlov, R. H. Baughman, S. J. Kim. Ultrafast charge and discharge biscrolled yarn supercapacitors for textiles and microdevices. *Nat. Commun*. 2013, **4**, 2970.

4. F. F. Liu, G. Y. Han, W. Z. Chang, D. Y. Fu, Y. P. Li, M.Y. Li. Fabrication of carbon nanotubes/polypyrrole/carbon nanotubes/melamine foam for supercapacitor. *J. Appl. Polym. Sci.* 2014,**131**, 39779.

5. M. L. Mao, L. Mei, L. C. Wu, Q. H. Li, M. Zhang. Facile synthesis of cobalt sulfide/carbon nanotube shell/core composites for high performance supercapacitors. *Rsc Advances* 2014, **4**, 12050-12056.

6. Y. B. Yang, P. X. Li, S. T. Wu, X. Y. Li, E. Z. Shi, Q. C. Shen, D. H. Wu, W. J. Xu, A. Y. Cao, Q. Yuan. Hierarchically designed three-dimensional macro/mesoporous carbon frameworks for advanced electrochemical capacitance storage. *Chem.—Eur. J*. 2015, **21**, 6157-6164.

7. Z. H. Ma, X. W. Zhao, C. H. Gong, J. W. Zhang, J. W. Zhang, X. F. Gu,; Tong, L. J. F. Zhou, Z. J. Zhang. Preparation of a graphene-based composite aerogel and the effects of carbon nanotubes on preserving the porous structure of the aerogel and improving its capacitor performance. *J. Mater. Chem. A* 2015, **3**, 13445-13452.

8. Y.C. Qiu, G.Z. Li, Y. Hou, Z. H. Pan, H. F. Li, W. F. Li, M. N. Liu, F. M. Ye, X.W. Yang, Y.G. Zhang. Vertically aligned carbon nanotubes on carbon nanofibers: a hierarchical three-dimensional carbon nanostructure for high-energy flexible supercapacitors. *Chem. Mater*. 2015, **27**: 1194-1200.

9. X. Xiang, W. J. Zhang, Z. P. Yang, Y. Y. Zhang, H. J. Zhang, H. Zhang, H. T Guo, X. T. Zhang, Q. W. Li. Smart and flexible supercapacitor based on a porous carbon nanotube film and polyaniline hydrogel. *Rsc Advances* 2016, **6**, 24946-24951.

10. W. Yang, L. He, X. Tian, M. Yan, H. Yuan, X. Liao, J. Meng, Z. Hao, L. Mai. Carbon-MEMS-based alternating stacked MoS_2@rGO-CNT micro-supercapacitor with high capacitance and energy density. *Small* 2017, 1700639.

11. Z. Li, Z. Li, L. Li, C. Li, W. Zhong, H. Zhang. Construction of hierarchically one-dimensional core-shell CNT@microporous carbon by covalent bond-induced surface-confined crosslinking for high-performance supercapacitor. *ACS Appl. Mater. Interfaces* 2017, **9** (18), 15557-15565.